Available online at www.sciencedirect.com
SCIENCE DIRECT®
Applied Surface Science 234 (2004) 107–112
applied surface science
www.elsevier.com/locate/apsusc

Barrier formation at metal–organic interfaces: dipole formation and the charge neutrality level

H. Vázquez[a,*], F. Flores[a], R. Oszwaldowski[a,b], J. Ortega[a], R. Pérez[a], A. Kahn[c]

[a]Departamento de Física Teórica de la Materia Condensada, Universidad Autónoma de Madrid, E-28049 Madrid, Spain
[b]Instytut Fizyki Mikołaja Kopernika, Grudziądzka 5, 87-100 Toruń, Poland
[c]Department of Electrical Engineering, Princeton University, Princeton, NJ 08544, USA

Available online 2 July 2004

Abstract

The barrier formation for metal–organic semiconductor interfaces is analyzed within the induced density of interface states (IDIS) model. Using weak chemisorption theory, we calculate the induced density of states in the organic energy gap and show that it is high enough to control the barrier formation. We calculate the charge neutrality levels of several organic molecules: 3,4,9,10-perylenetetracarboxylic dianhydride (PTCDA), 3,4,9,10-perylenetetracarboxylic bisbenzimidazole (PTCBI) and 4,4′,*N*,*N*′-dicarbazolyl biphenyl (CBP) and the interface Fermi level for their contact with a Au (1 1 1) surface. We find an excellent agreement with the experimental evidence and conclude that the barrier formation is due to the charge transfer between the metal and the states induced in the organic energy gap.

Keywords: Metal–organic interface; Charge neutrality level; Induced density of interface states; Energy level alignment; Barrier formation; Fermi level pining

1. Introduction

The field of electronic materials based on molecular films is developing very fast. Designing new organic-based materials and devices requires a detailed knowledge of basic processes, such as those controlling the formation of metal–organic interface barriers (see [1]).

The evolution of our understanding of this aspect of organic interfaces follows a path which reminds us of the slow process of understanding inorganic semiconductor–metal interfaces. Twenty-five years ago, the main problem was to understand the mechanism of the formation of the Schottky barrier. Starting with the Schottky and Bardeen models, research developed new ideas based on the Defect model [2] and the induced density of interface states model [3]. The present consensus on inorganic–metal interfaces is that, unless the interface has many defects, the Schottky barrier formation is controlled by ''intrinsic'' interface states induced by the interaction between the inorganic semiconductor and the metal.

Several models have been advanced to explain organic semiconductor–metal interface barrier formation. The Schottky–Mott model was originally believed to hold for these interfaces, assuming that no interface dipole is formed at the junction, a situation which was subsequently disproved in most cases (see [4,5]). At reactive interfaces, the metal-molecule

* Corresponding author.
E-mail address: hector.vazquez@uam.es (H. Vázquez).

0169-4332/$ – see front matter © 2004 Elsevier B.V. All rights reserved.
doi:10.1016/j.apsusc.2004.05.084

chemical reaction creates gap states that pin the Fermi level, a situation that is analogous to that described by the Unified Defect model proposed for inorganic semiconductor–metal interfaces [6]. Compression of the metal surface electronic tail by the organic molecules, leading to a change in the metal workfunction, has also been suggested as a mechanism operating in organic-metal interfaces [7].

This communication focuses on non-reactive interfaces between metals and thin films of low weight organic molecules. We study several organic semiconductor–metal interfaces within the IDIS model [3] and show that the induced densities of states at these junctions are large enough to control the interface barrier formation. We analyze the chemical interaction between Au and several organic molecules: 3,4,9,10-perylenetetracarboxylic dianhydride (PTCDA), 3,4,9,10-perylenetetracarboxylic bisbenzimidazole (PTCBI) and 4,4′,*N*,*N*′-dicarbazolyl biphenyl (CBP) (Fig. la). Our quantum-mechanical analysis shows how the weak chemical interaction creates, nevertheless, a local density of states in the organic energy gap, which is large enough to make the IDIS model applicable and the definition of a charge neutrality level (CNL) for the organic molecule meaningful. Our results for these junctions explain their pinning behaviour, which is characterized by the interface slope parameter, $S = dE_F/d\phi_M$. A low value of S (as is the case of PTCDA/Au and PTCBI/Au) corresponds to strong Fermi level pinning, whereas a higher value of S (CBP/Au is an example) means that the change of the barrier height with the metal workfunction is larger: as will be discussed below, this is associated with a smaller density of states induced in the organic energy gap.

2. Model and theoretical solution

Consider, initially, the case of a PTCDA–Au interface. Experimental evidence indicates that PTCDA molecules lie flat on the Au surface, and that the PTCDA monolayer has the two-dimensional pattern shown in Fig. 1b. PTCDA crystals can be thought of being formed by the repetition of this layer along the direction perpendicular to the surface [9]. It is important to realize that, as is typical of organic crystals, intermolecular bonds are weak van der Waals bonds that preserve the individuality of the molecules. This

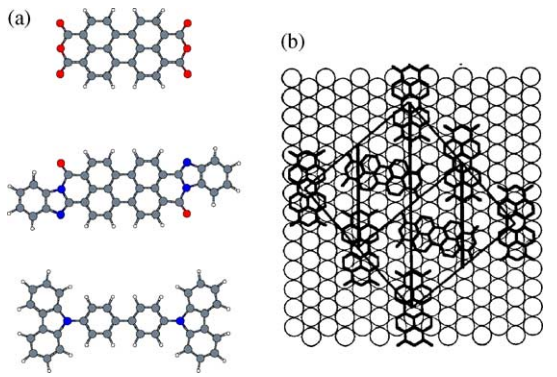

Fig. 1. (a) Organic molecules studied in this paper: PTCDA, PTCBI and CBP; (b) two-dimensional pattern of a PTCDA crystal (from [8]).

simplifies the analysis of the PTCDA–Au interaction, reducing it to the case of a single molecule deposited with its plane parallel to the surface.

We should stress that, in principle, the molecule–molecule interaction induces some (small) broadening of the electronic levels of each individual molecule, but does not create an electron density of states in the molecular energy gap. Since the Schottky barrier formation depends on these gap states, we can safely neglect the molecule–molecule interaction and consider only the single molecule–metal interaction.

Our analysis of the organic semiconductor–metal interface is made in several steps. First, the organic molecule is analyzed using a DFT-LCAO method [10]; this is a DFT-based theory, which uses a local-orbital basis and the orbital occupation for describing the exchange and correlation energies of the system. It has been shown elsewhere that this approach is equivalent to other more conventional DFT methods that use a local exchange and correlation energy [11].

The main problem with DFT methods for organic molecules (and other small molecules) is that their one-electron eigenvalues do not represent real electron or hole excitations. In particular, the DFT energy gap is not directly related to either the transport or the optical gap. The advantage of our approach is that, by using a variation of Koopman's theorem [11], we can calculate the molecular electronic levels by introducing a relaxation energy in the DFT method that is directly related to the exchange-correlation energy. We have shown for PTCDA [12] that, although this effect is important, the relaxation of the molecular

orbitals calculated within DFT is negligible [11]. This means that, after the DFT-LCAO calculation for the organic molecule, we need to renormalize the energy levels by means of Koopman's relaxation energies in order to obtain a realistic energy spectrum. We can keep, however, the electronic wavefunctions of the molecule obtained from the DFT calculation.

Fig. 2 illustrates this situation for PTCDA. Panel (a) shows the energy spectrum calculated within DFT-LCAO, while panel (b) shows the spectrum after introducing Koopman's relaxation energies. Note how the PTCDA energy gap increases from 1.6 to 5.7 eV due to these relaxation effects; the molecular wavefunctions associated with the ionization (HOMO) and affinity (LUMO) levels are assumed to be practically the same before and after the energy relaxation.

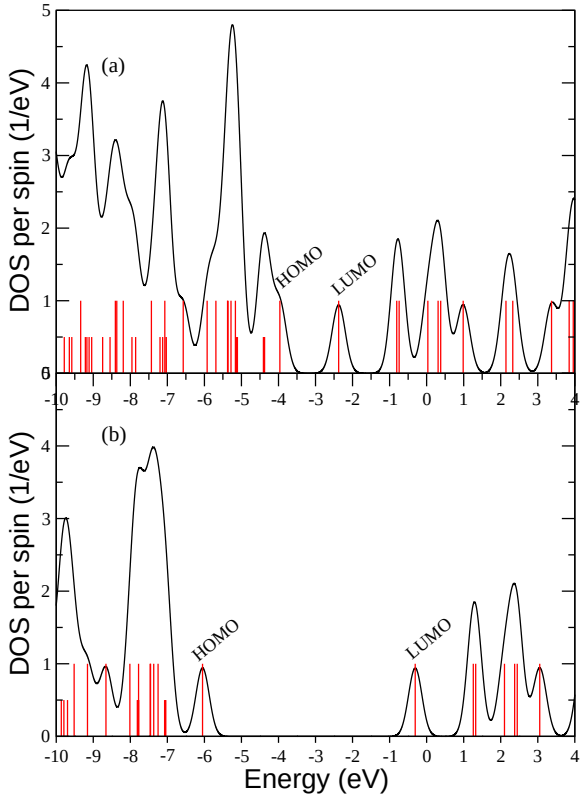

Fig. 2. DFT-LCAO energy spectrum (long bars: π-states; short bars: σ-states) before (a) and after (b) Koopman's relaxation energies; the relaxation in the wavefunctions, however, is small. The DOS is obtained by introducing a 0.5 eV FWHM Gaussian broadening for each level.

There are also solid-state effects associated with long-range electronic polarization. These are mainly associated with screening of the metal and the organic crystal of the electronic field created by the extra charge (electron or hole) introduced in the molecule [13]. This correction reduces the energy gap by $\sim$1.5 eV, although the ionization and affinity wavefunctions of the molecule are not expected to present important modifications. Other polarization effects, due to lattice relaxation and vibronic effects only introduce small corrections, around 0.2 eV, further reducing the molecular energy gap [6]. Regarding PTCDA, we fit the molecular transport gap to 3.2 eV, which presumably takes into account all the effects discussed above [6]; this is done by introducing a rigid shift between the empty and occupied states of Fig. 2b. For PTCBI and CBP, we fit the transport gaps to 3.1 and 5.1 eV respectively, values which were deduced from experimental optical gaps and exciton binding energies [14].

In a second step, we calculate the induced density of states at the organic semiconductor–metal interface using chemisorption theory in the limit of weak interaction between the two systems [16]. In our model, we assume the organic molecule (PTCDA, PTCBI or CBP) to be deposited flat on the metal surface, at a distance d from the last metal layer, which we will take for the rest of this paper to be Au (1 1 1).

In our analysis, we start with the organic molecule wavefunctions ψ_i, obtained from the DFT-LCAO method discussed above, and the metal density of states matrix, $\rho_{\alpha\beta}(E)$, where α and β refer to the local-orbital basis used to describe the metal properties, which are calculated using the DFT local-orbital code *Fireball* [15]. In the limit of weak PTCDA–metal interaction, the main effect of the metal is to broaden the molecular levels E_i by the quantity Γ_i [16]:

$$\Gamma_i = 2\pi \sum_v |T_{iv}|^2 \delta(E_v - E_i) \tag{1}$$

where T_{iv} is the hopping interaction between the molecular orbital ψ_i and the metal eigenfunction, ψ_v. Eq. (1) can be rewritten in a more convenient way by using the local-orbital basis for the molecule and the metal. Writing $\psi_i = \sum_j c_{ij}\phi_j$, Eq. (1) takes the form:

$$\Gamma_i = 2\pi \sum_{jj'\alpha\beta} c_{ij} T_{j\alpha} \rho_{\alpha\beta}(E_i) T_{\beta j'} c_{j'i} \tag{2}$$

Neglecting off-diagonal terms with $j \neq j'$ and $\alpha \neq \beta$, which tend to cancel each other out, Eq. (2) is further simplified to:

$$\Gamma_i = 2\pi \sum_{j,\alpha} |c_{i,j}|^2 |T_{j,\alpha}|^2 \rho_{\alpha,\alpha}(E_i) \tag{3}$$

In our calculation, we have only included the interaction of the Au 6s orbital with the different orbitals of the organic molecules, C 2s and 2p, N 2s and 2p, O 2s and 2p, and H 1s. This implies that in Eq. (3), α refers only to the Au 6s orbitals. Fig. 3 shows these interactions as a function of the Au-atom distance, which obviously depends on the organic–metal distance, d.

The organic-metal separation is a difficult issue. First, no experimental value exists for these systems. Second, conventional DFT codes cannot be used to calculate d, due to the weak van der Waals interaction between the metal and the organic molecule [9]. Using indirect information based on: (a) the PTCDA–PTCDA stacking distance, $d \sim 3.2$ Å, and (b) the atomic radius of Au (~0.5 Å larger than that of C), we assume the distances between the last Au layer and the plane of the organic molecules considered in this paper to be around 3.5 ± 0.3 Å. We make use of this value to calculate Γ_i from Eq. (3).

Once Γ_i is calculated, each molecular level E_i contributes to the organic LDOS with the Lorentzian function

$$\frac{1}{\pi} \frac{\Gamma_i/2}{(E - E_i)^2 + (\Gamma_i/2)^2} \tag{4}$$

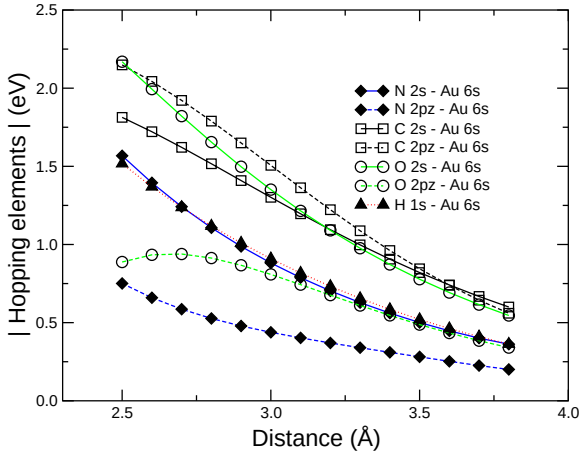

Fig. 3. Hopping elements between the atoms which make up the organic molecule and Au as a function of distance.

The total LDOS is obtained by adding all the contributions from the different molecular orbitals.

3. Results and conclusions

Fig. 4 shows our results for PTCDA, PTCBI and CBP. In these calculations $d = 3.5$ Å, $\Gamma_i^{\pi} \simeq 0.5$ and $\Gamma_i^{\sigma} \simeq 0.25$ eV. Note the different broadening of the π and σ levels. These values were obtained using Eq. (3) and the hopping integrals of Fig. 3 for $d = 3.5$ Å. Note also the uncertainty on the broadening, due to the uncertainty in the metal–organic distance (see below).

Fig. 4 shows the different molecular levels for each molecule, the π-(σ-) states being drawn as long (short) bars. For each molecule, the CNL is calculated by imposing charge neutrality conditions: the total electronic charge below the CNL integrates to the number of occupied molecular states. Table 1 shows the calculated CNLs (measured from the ionization level). Also included in this table are the transport gaps for the sake of comparison. Note the similarity between PTCDA and PTCBI, with the CNL level rather close to the affinity level. This is due to the similarity of their energy spectra and transport gaps. In both cases the CNL is close to the affinity level because of the distribution of 7π-states around the energy gap. The large density of states below the ionization level pushes the CNL upper in the gap. For CBP, the CNL is closer to the molecular midgap, due to the larger energy gap and the more symmetric distribution of π-states around the HOMO and LUMO.

The interface slope parameter, $S = dE_F/d\phi_M$, is given by:

$$S = \frac{dE_F}{d\phi_M} = \frac{1}{1 + 4\pi e^2 D(E_F)\delta/A} \tag{5}$$

where $D(E_F)$ is the induced density of states at the Fermi energy (twice the values shown in Fig. 4), d the

Table 1
Charge neutrality levels (measured from the center of the HOMO) and peak-to-peak transport gaps, for the three organic materials

	CNL (eV)	E_g^t (eV)
PTCDA	2.5	3.2
PTCBI	2.4	3.1
CBP	3.0	5.1

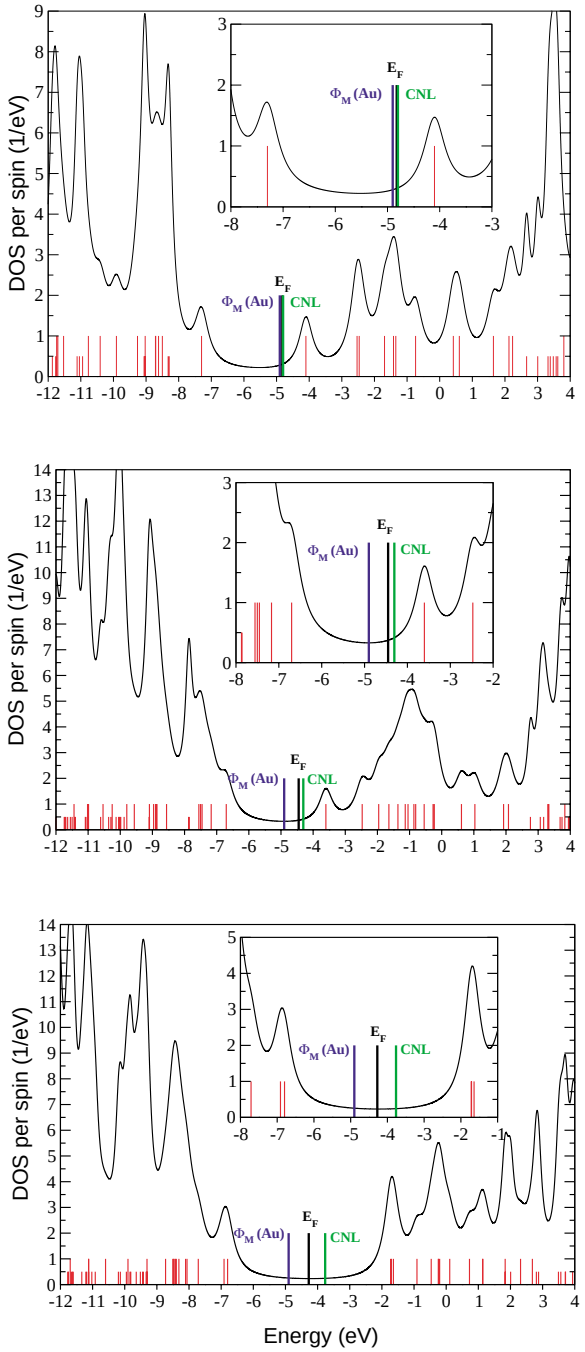

Fig. 4. (Top to Bottom:) IDIS, CNL and interface Fermi level for PTCDA/Au, PTCBI/Au and CBP/Au. Long (short) bars correspond to the π-(σ)-states neglecting the metal–molecule interaction. The insets show the region around E_F in detail.

Table 2
Calculated and experimental values for the interface slope parameter, S

	PTCDA/Au	PTCBI/Au	CBP/Au
S(theory)	0.2	0.2	0.5
S(exp)	0.0	0.0	0.6

metal–organic distance and A the area associated with one organic molecule (see Fig. 1; $A = 120$, 191 and 251 Å^2, for PTCDA, PTCBI and CBP, respectively). Table 2 compares the experimental and calculated values for the slope parameter. Note again the similarity between PTCDA and PTCBI, and the larger value found for CBP. This is due to the smaller $D(E_F)$ and the larger area A. The different pinning behaviour of the three interfaces is explained: the low value of S, as is the case of PTCDA and PTCBI on Au (1 1 1), corresponds to a high pinning at the organic CNL. For CBP/Au (1 1 1), on the other hand, the larger value of S reflects the higher ability of E_F to move within the organic energy gap.

This can be seen in the relation $\mathrm{CNL} - E_F = S(\mathrm{CNL} - \phi_M)$. Having calculated CNL and S, we obtain the interface Fermi level straightforwardly. The pinning at the interface reduces the initial difference $\mathrm{CNL} - \phi_M$, to the injection barrier $E_F - \phi_M$.

Fig. 4 also shows the position of the Fermi level for interfaces with Au. The position, measured from the ionization level, is shown for each molecular film in Table 3. The agreement between the theoretical and experimental positions of E_F and values of S is remarkable, although a small difference appears for the slope parameter. This presumably reflects the approximations introduced in our calculation. The main source of inaccuracy comes from the assumed value of d, which has an error bar of around ± 0.3 Å. This inaccuracy is mainly reflected in the calculated values of $D(E_F)$, while the CNL is probably very insensitive to that modification. To ascertain this point,

Table 3
Theoretical and experimental interface Fermi level positions, measured from the center of the HOMO

	PTCDA/Au	PTCBI/Au	CBP/Au
E_F (theory) (eV)	2.5	2.3	2.5
E_F (exp)	2.5	2.1	2.4

we recalculated the CNL changing Γ_i^{π} and Γ_i^{σ} by factors of up to 2, and found that its value remains practically the same. This is not the case for $D(E_F)$, which changes by 50% when d changes ± 0.2 Å. Our results suggest that d has probably been overestimated for PTCDA and PTCBI by at least 0.3 Å in our calculations.

We stress, however, that our results for the interface Fermi level show very good agreement with the experimental data. Moreover, the main outcome of our analysis is to show that the induced density of interface states is large enough to play a crucial role in the formation of the metal–organic semiconductor barriers. This allows us to conclude that the mechanism associated with the formation of these interface barriers is the charge transfer between the two materials due to the weak chemical interaction: this creates an electrostatic interface dipole which tends to align the metal Fermi level and the organic CNL.

Acknowledgements

We gratefully acknowledge financial support by the Consejería de Educacion de la Comunidad de Madrid, the Spanish CICYT under project MAT 2001-0665, and the DIODE network (HPRN-CT-1999-00164). Support of this work by the National Science Foundation (DMR-0097133) and the New Jersey Center for Organic Optoelectronics (AK) is also acknowledged.

References

[1] H. Ishii, K. Seki, in: W. Salaneck et al., (Eds.), Conjugated Polymer and Molecular Interfaces, Dekker, 2001, pp. 293–349.
[2] W.E. Spicer, et al., Appl. Surf. Sci. 41 (1989) 1.
[3] C. Tejedor, E. Louis, F. Flores, J. Phys. C 10 (1977) 2163; W. Mönch, Surf. Sci. 299 (1994) 928.
[4] C. Schen, A. Kahn, in: W. Salaneck et al., (Eds.), Conjugated Polymer and Molecular Interfaces, Dekker, pp. 351–400.
[5] S. Narioka, et al., Appl. Phys. Lett. 67 (1995) 1899; I.G. Hill, et al., Appl. Phys. Lett. 73 (1998) 662.
[6] C. Schen, J. Schwartz, A. Kahn, J. Appl. Phys. 89 (2001) 449.
[7] H. Ishii, et al., Adv. Mater. 11 (1999) 605.
[8] P. Fenter, et al., Phys. Rev. B 56 (1997) 3046.
[9] S. Forrest, Chem. Rev. 97 (1997) 1793.
[10] P. Pou, et al., Phys. Rev. B 62 (2000) 4309.
[11] R. Oszwaldowski, et al., J. Phys: Condensed Matter 15 (2003) S2665.
[12] H. Vázquez et al., Europhys. Lett. 65 (2004) 802.
[13] E.V. Tsiper, et al., Chem. Phys. Lett. 360 (2002) 47.
[14] I.G. Hill, et al., Org. El. 1 (2000) 5; I.G. Hill, et al., J. Appl. Phys. 84 (1998) 3236.
[15] J.P. Lewis, et al., Phys. Rev. B 64 (2001) 195103.
[16] A. Zangwill, Physics at Surfaces, Cambridge University Press, 1988.